Eur. Phys. J. B **29**, 61–69 (2002)
DOI: 10.1140/epjb/e2002-00262-2

THE EUROPEAN PHYSICAL JOURNAL B

Electronic structure of $LaNi_5$ and its hydride $LaNi_5H_7$

H. Zheng[1,a], Y. Wang[2], and G. Ma[2]

[1] Pohl Institute of Solid State Physics, Tongji University, Shanghai 200092, PR China
[2] Beijing Institute of Applied Physics and Computational Mathematics, Beijing 100088, PR China

Received 13 July 2001 / Received in final form 10 December 2001
Published online 17 September 2002 –

Abstract. The electronic structure of $LaNi_5$ and its hydride $LaNi_5H_7$ are obtained using the self-consistent cluster-embedding calculation method. The Fermi level of $LaNi_5H_7$ is 5.172 eV higher than that of $LaNi_5$. In both materials, the La 5*d* electrons locate nearby the Fermi levels, and make only a small contribution to the density of states (DOS) of the valence bands. There is no significant charge transfer from La to Ni in $LaNi_5$. But for $LaNi_5H_7$, there is a charge transfer of 1.16 electrons from La to H, and H atoms are combined mainly with Ni to form hybridized orbitals in the energy regions far below the Fermi level. An explanation of hydrogenation of $LaNi_5$ is proposed: It is easy for hydrogens to take off some localized La 5*d* electrons near the Fermi level, and combine with Ni to form hybridized orbitals in lower energy regions. This process is therefore in favor of energy, and forces a lattice expansion until the Fermi level rises to zero.

PACS. 71.20.-b Electron density of states and band structure of crystalline solids – 71.28.+d Narrow-band systems; intermediate-valence solids – 71.15.-m Methods of electronic structure calculations

1 Introduction

The hydrogen storage material $LaNi_5$ has attracted considerable attention [1]. It is generally believed that two factors, the size factor and the electronic factor, control a metal's solvent power for hydrogen. The former has been stressed by Lundin *et al.* [2]. The latter is related to the bonding of hydrogen to the metal lattice. Hydrogen is absorbed dissociatively. The cleavage of the hydrogen bond is endothermal to the extent of about 4.45 eV/H_2. So there must be a strong exothermal interaction with the lattice as hydrogen enters to compensate for this energy. In order to understand the hydrogenation, first, we must know the electronic structure. Due in part to the complexity of the crystal structure and the controversy concerning the location of hydrogen in $LaNi_5$, as we know, there are only two calculations for $LaNi_5$ [3,4] and one calculation for $LaNi_5H_7$ [4]. The APW (augmented plane wave) band structure calculation, performed by Malik *et al.* [3], does not contain the correlation potential, and its exchange potential is of the Slater Xα type with $\alpha = 1$. For the calculations of Gupta [4], the Hamiltonian includes only the *s* and *d* functions at the transition metal site, and it is not clear whether the calculations are spin-polarized. Up to today, the interaction of hydrogen with $LaNi_5$ lattice has not been elucidated in any more than the most general terms; such as, for example, to assert that there is a strong La-H affinity in the $LaNi_5$ hydride, etc.

[a] e-mail: zhenghp@mail.tongji.edu.cn

The self-consistent cluster-embedding (SCCE) calculation method is developed by the author [5,6] based on density functional theory, and is a first-principle method. Unlike the band structure calculation and free-cluster calculation, the SCCE calculation uses a set of localized non-interacting electrons to describe systems. It has been successfully applied to transition-metal monoxides NiO, CoO, pure Ni and hydrogen-decorated vacancies in Ni [5,7,8]. Recently, the electronic structure of a biological macromolecule, the trypsin inhibitor from squash seeds (CMTI-I), is obtained by the SCCE calculations [9]. In this paper, the electronic structures of $LaNi_5$ and $LaNi_5H_7$ are obtained by first-principle, all electron, full potential calculations using the SCCE method. A new explanation of hydrogenation of $LaNi_5$ is proposed. In Section 2, we outline briefly the theoretical method. The results are presented in Sections 3 and 4, and summarized in Section 5.

2 Theoretical model

Although the self-consistent cluster-embedding (SCCE) calculation method has been described in detail elsewhere [6,9], we provide a brief overview for completeness.

In the density functional theory (DFT) [10], Kohn and Sham assume that a non-interacting electron system has the same ground-state charge density as the real interacting system [11]. Thus the energy function of a system containing N electrons and M fixed nuclei can be written

as (no relativistic effect is included; atomic units are used throughout this paper: $e^2 = 2$, $\hbar = 1$, $2m_e = 1$):

$$E_v[\rho] = T_{ni}[\rho] + E_{xc}[\rho] + \int\int \frac{\rho(\mathbf{r})\rho(\mathbf{r}')}{|\mathbf{r}-\mathbf{r}'|}\mathrm{d}\mathbf{r}\mathrm{d}\mathbf{r}' - 2\sum_{j=1}^{\mathrm{M}} \int \frac{\rho(\mathbf{r})Z_j}{|\mathbf{r}-\mathbf{R}_j|}\mathrm{d}\mathbf{r} + \sum_{i\neq j}^{\mathrm{M}} \frac{Z_i Z_j}{|\mathbf{R}_i - \mathbf{R}_j|}, \quad (1)$$

where $T_{ni}[\rho]$ is the kinetic energy of a non-interacting electron system. In the local spin density approximation (LSDA), the exchange-correlation energy $E_{xc}[\rho]$ is

$$E_{xc}[\rho] = \int \rho(\mathbf{r})\epsilon_{xc}(\rho^{up}(\mathbf{r}), \rho^{down}(\mathbf{r}))\mathrm{d}\mathbf{r}. \quad (2)$$

Each non-interacting electron can now be represented by a *stationary state* one-electron wave function $\phi_n^\sigma(\mathbf{r})$. The total $\rho(\mathbf{r})$ and $T_{ni}[\rho]$ are the sums of the electronic density and kinetic energy of each non-interacting electron, respectively.

$$\rho(\mathbf{r}) = \rho^{up}(\mathbf{r}) + \rho^{dn}(\mathbf{r}) = \sum_{occupied\ l} |\phi_l^{up}(\mathbf{r})|^2 + \sum_{occupied\ m} |\phi_m^{dn}(\mathbf{r})|^2 \quad (3)$$

$$T_{ni}[\rho] = \sum_{occupied\ l} \int \phi_l^{up*}(\mathbf{r})(-\nabla^2)\phi_l^{up}(\mathbf{r})\mathrm{d}\mathbf{r} + \sum_{occupied\ m} \int \phi_m^{dn*}(\mathbf{r})(-\nabla^2)\phi_m^{dn}(\mathbf{r})\mathrm{d}\mathbf{r}. \quad (4)$$

Using formulae (2, 3) and (4), the single-electron Schrödinger equation, *i.e.*, the well-known Kohn-Sham equation [11], can be obtained by the variation of function (1) with respect to $\phi_n^{\sigma*}(\mathbf{r})$ under the conservation rule $\int \rho(\mathbf{r})\mathrm{d}\mathbf{r} = N$:

$$\left\{-\nabla^2 + 2\int \frac{\rho(\mathbf{r}')}{|\mathbf{r}-\mathbf{r}'|}\mathrm{d}\mathbf{r}' - 2\sum_{i=1}^{\mathrm{M}} \frac{Z_i}{|\mathbf{r}-\mathbf{R}_i|} + V_{xc}^\sigma(\mathbf{r})\right\} \times \phi_n^\sigma(\mathbf{r}) = \epsilon_n^\sigma \phi_n^\sigma(\mathbf{r}). \quad (5)$$

The variation of equation (1) requires no restriction on the trial one-electron wave functions $\phi_n^\sigma(\mathbf{r})$. In the actual calculation of equation (5), however, it is impossible to have the $\phi_n^\sigma(\mathbf{r})$ unrestricted. What we can do is to use two kinds of non-interacting electrons to describe the real system approximately. They satisfy different boundary conditions, and correspond to different calculation methods.

2.1 Spread non-interacting electron model

Each one-electron wave function $\phi_n^\sigma(\mathbf{r})$ is assumed to spread over the whole region occupied by the system. Under this model, equation (5) can be used for free-cluster calculations with the natural finite boundary condition $\phi_n^\sigma(\mathbf{r}) \overset{|\mathbf{r}|\to\infty}{\longrightarrow} 0$, or for band structure calculations with periodic boundary condition.

2.2 Localized non-interacting electron model

Each one-electron wave function $\phi_n^\sigma(\mathbf{r})$ is assumed to be distributed in a part of the region occupied by the system. Under this model, equation (5) is used for self-consistent cluster-embedding (SCCE) calculation [6]: The N $\phi_n^\sigma(\mathbf{r})$ are divided into several groups. The $\phi_n^\sigma(\mathbf{r})$ in different groups will satisfy different special boundary conditions, and localize in different regions. The details are as follows.

The system can be divided into k embedded-clusters. For each embedded-cluster (whose electronic density is represented by $\rho_1(\mathbf{r})$), the rest of the system is treated as an environment with electronic density $\rho_2(\mathbf{r})$ which has a small overlap with the $\rho_1(\mathbf{r})$. Because all N $\phi_n^\sigma(\mathbf{r})$ are localized, we have ($N = N_1 + N_2$):

$$\begin{aligned}\rho(\mathbf{r}) &= \sum_{occupied\ n\ \sigma}^{\mathrm{N}} |\phi_n^\sigma(\mathbf{r})|^2 \\ &= \sum_{occupied\ n_1\ \sigma}^{\mathrm{N}_1} |\phi_{n_1}^\sigma(\mathbf{r})|^2 + \sum_{occupied\ n_2\ \sigma}^{\mathrm{N}_2} |\phi_{n_2}^\sigma(\mathbf{r})|^2 \\ &\equiv \rho_1(\mathbf{r}) + \rho_2(\mathbf{r}). \end{aligned} \quad (3b)$$

$$\begin{aligned}T_{ni}[\rho] = T_{ni}[\rho_1 + \rho_2] &= \sum_{occupied\ n\ \sigma}^{\mathrm{N}} \int \phi_n^{\sigma*}(\mathbf{r})(-\nabla^2)\phi_n^\sigma(\mathbf{r})\mathrm{d}\mathbf{r} \\ &= \sum_{occupied\ n_1\ \sigma}^{\mathrm{N}_1} \int \phi_{n_1}^{\sigma*}(\mathbf{r})(-\nabla^2)\phi_{n_1}^\sigma(\mathbf{r})\mathrm{d}\mathbf{r} \\ &\quad + \sum_{occupied\ n_2\ \sigma}^{\mathrm{N}_2} \int \phi_{n_2}^{\sigma*}(\mathbf{r})(-\nabla^2)\phi_{n_2}^\sigma(\mathbf{r})\mathrm{d}\mathbf{r} \\ &\equiv T_{ni}[\rho_1] + T_{ni}[\rho_2]. \end{aligned} \quad (4b)$$

A *zero-value* term $\int \rho_1(\mathbf{r})V_{or}\mathrm{d}\mathbf{r}$ is added to the right side of formula (1). For fixed $\rho_2(\mathbf{r})$, using formulae (2), (3b) and (4b), the variational principle now leads to the basic equation of the SCCE method [6]:

$$\left\{-\nabla^2 + 2\int \frac{\rho_1(\mathbf{r}') + \rho_2(\mathbf{r}')}{|\mathbf{r}-\mathbf{r}'|}\mathrm{d}\mathbf{r}' - 2\sum_{i=1}^{\mathrm{M}} \frac{Z_i}{|\mathbf{r}-\mathbf{R}_i|} + V_{xc}^\sigma(\mathbf{r}) + V_{or}(\mathbf{r})\right\}\phi_n^\sigma(\mathbf{r}) = \epsilon_n^\sigma \phi_n^\sigma(\mathbf{r}), \quad (5b)$$

where the $\phi_n^\sigma(\mathbf{r})$ represent only the non-interacting electrons localized in and around the embedded-cluster. For a real finite system, by calculating all k embedded-clusters one by one, equation (5b) gives a complete set of one-electron eigenfunctions of the whole system which makes the total energy in formula (1) a minimum.

The $V_{or}(\mathbf{r})$ is defined as

$$V_{or}(\mathbf{r}) = \begin{cases} 2\sum_{j=1}^{\mathrm{M}_2} \frac{Z_j}{|\mathbf{r}-\mathbf{R}_j|} & \text{if } \mathbf{r} \text{ is in the core regions of surrounding atoms} \\ 0 & \text{otherwise,} \end{cases} \quad (6)$$

where the M_2 is the number of surrounding atoms. In the calculations, the $V_{or}(\mathbf{r})$ cancels the nuclear Coulomb potential in the core regions of all surrounding atoms. The cluster-electrons will only feel an electron-electron positive Coulomb potential in these regions and be forced out. So the $\phi_n^\sigma(\mathbf{r})$ in equation (5b) satisfy a special boundary condition caused by the $V_{or}(\mathbf{r})$:

$$\phi_n^\sigma(\mathbf{r})|_{\mathbf{r} \text{ is in the core regions of surrounding atoms}} = 0. \quad (7)$$

The physical reasons for the boundary condition (7) are given in reference [6]. In addition, there is a special finite boundary condition for $\phi_n^\sigma(\mathbf{r})$ because of its locality:

$$\phi_n^\sigma(\mathbf{r}) \overset{\mathbf{r} \text{ gradually go away from the embedded cluster}}{\longrightarrow} 0. \quad (8)$$

It is achieved by using pre-localized wave functions, *i.e.*, each $\phi_n^\sigma(\mathbf{r})$ is expanded into a set of localized basis functions which are not zero only in and around the embedded cluster region.

Now we show that equation (5b) is just the Kohn-Sham equation (5) with special boundary conditions. Apparently, the equation (5b) is exactly the same as the Kohn-Sham equation (5) except for the "orthogonality constraint" $V_{or}(\mathbf{r})$. Look at the formula (6), it is easy to see that as long as the boundary condition (7) is satisfied, we have $\int \rho_1(\mathbf{r}) V_{or}(\mathbf{r}) \mathrm{d}\mathbf{r} = 0$. So the $V_{or}(\mathbf{r})$ in equation (5b) has no contribution to total energy, and the SCCE calculation is valid according to the DFT. The only effect of the $V_{or}(\mathbf{r})$ is to cause the special boundary condition (7). In fact, what we have done is transform the boundary condition (7) into an equivalent potential $V_{or}(\mathbf{r})$ in equation (5b). So equation (5b) is just the Kohn-Sham equation (5) with the special boundary condition (7) and (8). Note, the boundary conditions (7) and (8) are related to the position and surrounding atoms of the embedded cluster. The two boundary conditions are different for different embedded clusters which have different positions and surrounding atoms. In fact, we use the same Hamiltonian as the Kohn-Sham equation (5), but different boundary conditions to solve k sets of $\phi_n^\sigma(\mathbf{r})$, localized in different embedded cluster regions. Because the expansion bases of $\phi_n^\sigma(\mathbf{r})$, and the equivalent potential $V_{or}(\mathbf{r})$, are different for different embedded clusters, we may say that the effective Hamiltonians of k sets of $\phi_n^\sigma(\mathbf{r})$ are different.

There are two technique explanations for the actual SCCE calculation.

(A) The optimum values of core radii of surrounding atoms are determined according to two criteria: (i) there is no collapse disaster; (ii) the total cluster-electrons remaining in the surrounding core regions are minimum. In general, the boundary condition (7) can be satisfied with high precision, and it is found that the results are not sensitive to the core radii if they are around the optimum values.

(B) For a periodic crystal, only one embedded-cluster needs to be calculated self-consistently, while the $\rho_2(\mathbf{r})$ is identical with the periodic extension of $\rho_1(\mathbf{r})$. The periodical crystal potential can be well described by enough environmental atoms no matter what size the embedded-cluster is.

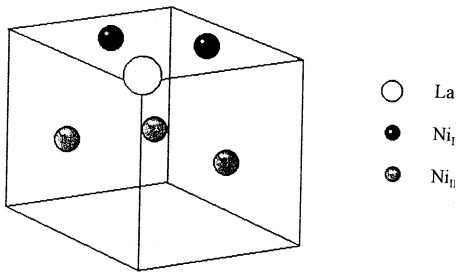

Fig. 1. The embedded-cluster of $LaNi_5$

3 Results of $LaNi_5$

$LaNi_5$ crystallizes within the $CaCu_5$ structure with space group P6/mmm [12]. Figure 1 shows the embedded-cluster of $LaNi_5$ which is surrounded by 156 atoms to simulate the α-phase crystal $LaNi_5$. The lattice constants used in our calculation are $a_o = 5.023$ Å, $c_o = 3.984$ Å [13,14]. The original optimized Gaussian bases of Ni and La are taken [15–18]. Then part of the bases are uncontracted and several diffuse bases are added. The final basis sets are: Ni – $10s6p6d$ which is contracted from $16s10p7d$; La – $14s10p7d$ which is contracted from $20s16p11d$. An isolated lanthanum atom has no $4f$ electron, and it is expected that lanthanum may lose electrons in both $LaNi_5$ and $LaNi_5H_7$. So only the configuration $4f^0$ of La is considered, and no f basis is used. The total number of Gaussian bases of the embedded-cluster $LaNi_5$ is 369. There are 901419 grid points used for numerical calculation of V_{xc}. After several trial calculations, the optimum values of core radii of surrounding La and Ni atoms are: $R_{\mathrm{La}} = 1.6861$ a.u., $R_{\mathrm{Ni}} = 0.7869$ a.u. The total number of cluster electrons remaining in the core regions of 156 surrounding atoms are 0.0005, which shows that the special boundary condition (7) is well satisfied.

Figure 2 shows the DOS of La-d, Ni-d, Ni-s, Ni-p and total electrons, where each single level has been broadened by a Gaussian function with a full width at half-maximum (FWHM) of 1 eV (s electrons), 0.5 eV (p electrons) and 0.3 eV (d electrons), respectively. The contribution of La-s and La-p electrons are negligible.

The results show that the Fermi level $E_F = -5.125$ eV, falls in a rapidly decreasing portion of the nickel $3d$ bands which are not fully filled. Below the Ni $3d$ bands, there are two Ni s-d hybridized bands centered at -9.0 eV and -10.2 eV, respectively. The La-$5p$ electrons locate in much lower energy regions, -21.935 eV to -25.824 eV, so they are not valence electrons. The valence bands, mainly contributed by nickel $3d$ electrons, contain Ni-$4s$ (6.66%), Ni-$3p$ (3.77%) and La-$5d$ (4.49%) electrons. The full width at half maximum (FWHM) of the nickel $3d$ bands is about 3.0 eV. Our calculations agree with the photoemission data [19,20] which show the occupied bands of $LaNi_5$ and a FWHM of 3.0 eV of nickel $3d$ bands. Besides, the data in Figure 2 can be used to calculate the electronic specific-heat coefficient $\gamma = \frac{\pi^2 k_B^2}{3} N(E_F)$. $N(E_F)$ is calculated to be $13.7 \times 6.022 \times 10^{23}$ (eV)$^{-1}$ (mole $LaNi_5$)$^{-1}$. From this, γ is evaluated to be 3.23×10^{-2} J (mole $LaNi_5$)$^{-1}$ K^{-2}.

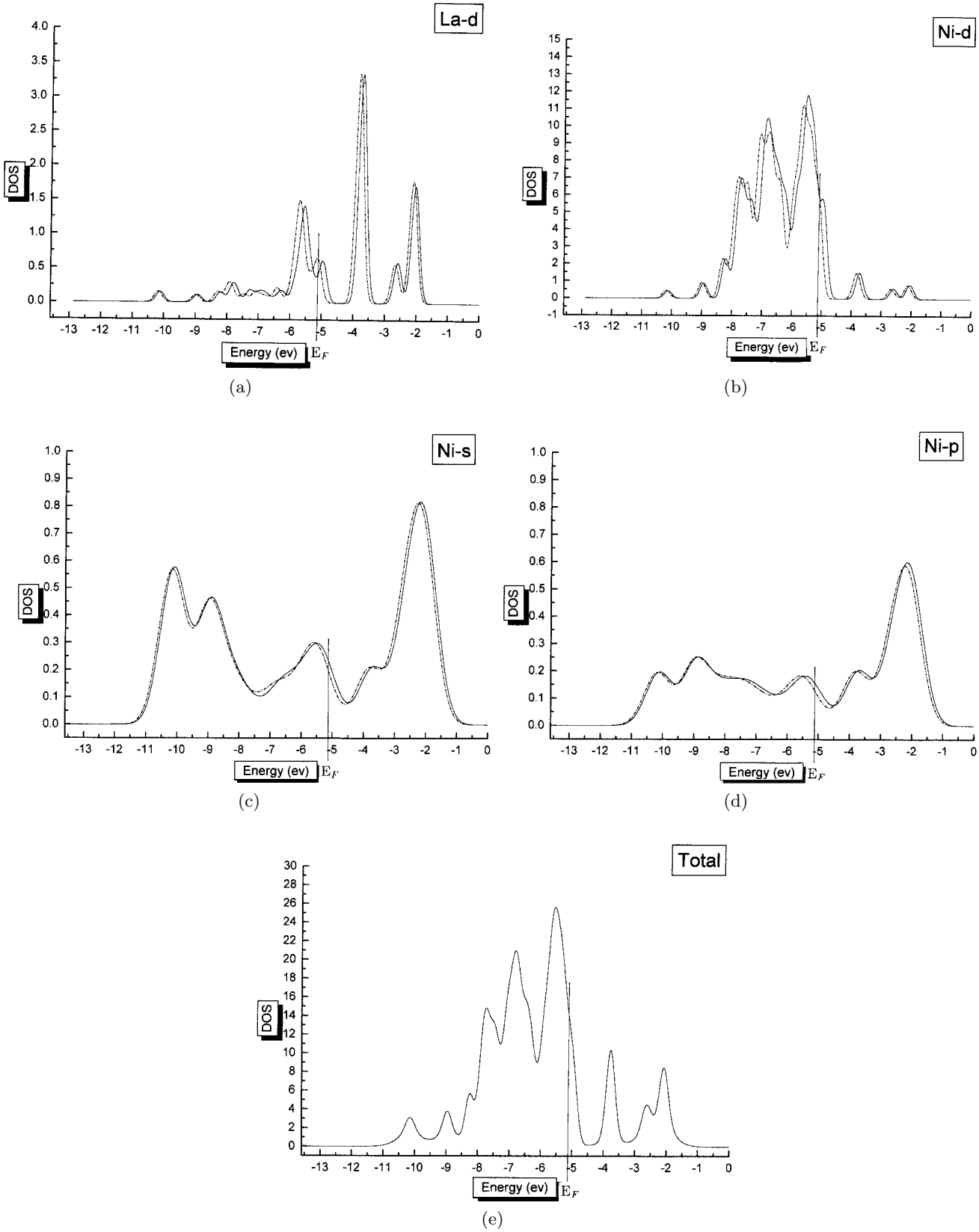

Fig. 2. Density of states of classified electrons of $LaNi_5$. Units of the DOS are states of per electron-volt per $LaNi_5$ cell. Dashed line: spin-up electrons. Solid line: spin-down electrons. (a) La-*d* electrons; (b) Ni-*d* electrons; (c) Ni-*s* electrons; (d) Ni-*p* electrons; (e) Total, the solid line including both spin-up and spin-down electrons.

This is to be compared with the experimental values in J mole^{-1} K^{-2} of 3.43×10^{-2} by Nasu *et al.* [21], 3.65×10^{-2} by Takeshita *et al.* [22], and 4.26×10^{-2} by Ohlendorf *et al.* [23]. The agreement with the SCCE calculations is seen to be quite good. Our results are in general agreement with the previous calculations [3,4], but there are three important differences.

(A) Our calculations reveal no significant charge transfer from La to Ni which is in agreement with the experimental data [20]: each La atom loses about 0.457 electrons, each Ni_I atom gets about 0.011 electrons, each Ni_{II} atom gets about 0.145 electrons. But the calculations of Malik *et al.* [3] show a charge transfer of 1.5 electrons from La to Ni. Gupta did not give this information [4].

(B) Our results show that the La atom has 2.53 $5d$ electrons hybridized with valence electrons of Ni. The La $5d$ electrons have a contribution of 10% to the DOS at E_F, and locate mostly near the Fermi level (in about 1 eV of energy region, see Fig. 2a). While the results of Gupta show that the contribution of lanthanum d states at E_F is almost nil [4].

(C) In our calculations, both majority-spin and minority-spin Ni $3d$ subbands are not fully filled which is in agreement with experiments. Whereas the calculations of Malik show an almost filled minority-spin band [3].

The Mulliken population analyses show 1 μ_B spin magnetic moment per formula unit: 0.221 μ_B for La, 0.069 μ_B for each Ni_I, 0.213 μ_B for each Ni_{II}, and all moments are parallel. Thus, $LaNi_5$ is a weak ferromagnet. The results of Malik are similar but each $LaNi_5$ cell has spin magnetic moment of 0.69 μ_B which is almost entirely due to the nickel [3]. No magnetic information has been given by Gupta's calculations [4]. However, all calculations above conflict with experimental data: $LaNi_5$ is reported to be an almost ferromagnetic Stoner enhanced Pauli paramagnet [24,25]. A possible reason is that the neighbor $LaNi_5$ cell may have opposite spin magnetic moment.

Finally, it may be worth discussing two points: For $LaNi_5$, why are the outcomes of the SCCE calculation and those of band structure calculations different? Which one is better?

Because the questions concern several fundamental concepts, we give step-by-step discussions.

(I) In the viewpoint of physics, the symmetry and distribution region of a single electron can be different from that of system Hamiltonian. First, the experiments have shown that a crystal can contain both periodic quasi-free electrons and non-periodic localized electrons. Second, in a many-electron Schrödinger equation

$$H\Psi_G(X1,\cdots,X_N) = E_G\Psi_G(X1,\cdots,X_N), \qquad (9)$$

the symmetry and distribution region of the total Hamiltonian H put restrictions only on the total wave function $\Psi_G(X1,\cdots,X_N)$. It does not require that a single electron must have the same symmetry and distribution region. Finally, the density functional theory concerns only the total electronic density and energy of a many-electron system. When Kohn and Sham introduce the non-interacting electron system from the viewpoint of total energy, they only assume that the non-interacting and interacting systems have the same ground-state charge density. So in equation (1), there is no reason to require that the symmetry and distribution region of every $|\phi_n^\sigma(\mathbf{r})|^2$ must be the same as that of $\rho(\mathbf{r})$.

(II) From the viewpoint of mathematics, the symmetry and distribution region of a single $|\phi_n^\sigma(\mathbf{r})|^2$ in equations (1) and (5) can be different from that of system $\rho(\mathbf{r})$. Assume the $E_{xc}[\rho]$ to be exact, so that equation (1) is exact. However, the variation of function (1) is exact only if the trial one-electron wave function $\phi_n^\sigma(\mathbf{r})$ is unrestricted. This means that there are two requirements in solving the Kohn-Sham equation (5): (i) $\phi_n^\sigma(\mathbf{r})$ must be expanded by a complete set of infinite number of basis functions. (ii) $\phi_n^\sigma(\mathbf{r})$ can have any kind of boundary condition, *i.e.*, a single $|\phi_n^\sigma(\mathbf{r})|^2$ can have any symmetry and distribution region (so it can be different from that of system $\rho(\mathbf{r})$). The reason for the requirement (ii) is simple: Any function can be expanded by a complete set of infinite number of basis functions. But a $\phi_n^\sigma(\mathbf{r})$, expanded by a complete set of infinite number of basis functions, is restricted if it is required to satisfy a certain boundary condition. If the requirements (i) and (ii) were satisfied, the variation of function (1) would give a unique set of $\{\phi_n^\sigma(\mathbf{r})\}$ corresponding to a unique correct $\rho(\mathbf{r})$. So the variation of function (1) with respect to $\phi_n^{\sigma*}(\mathbf{r})$ would be equivalent to the variation with respect to $\rho(\mathbf{r})$. Every real electron could be well described by a $\phi_n^\sigma(\mathbf{r})$ no matter what kind is the real electron. In this sense, the concept of "non-interacting electron system" is no longer important. As an example, consider a periodic crystal. If the crystal contains only quasi-free electrons, the $\{\phi_n^\sigma(\mathbf{r})\}$ would be Bloch functions. If the crystal contains only localized electrons, all $\phi_n^\sigma(\mathbf{r})$ would be localized. If the crystal contains both quasi-free and localized electrons, the $\{\phi_n^\sigma(\mathbf{r})\}$ would contain both Bloch functions and localized functions.

(III) Errors in actual calculations. To get actual solutions of equation (5), $\phi_n^\sigma(\mathbf{r})$ can only be expanded into a set of finite number of basis functions, and satisfy a certain boundary condition. So the trial one-electron wave function $\phi_n^\sigma(\mathbf{r})$ is restricted. Many different sets of $\{\phi_n^\sigma(\mathbf{r})\}$ can now be used to get approximate $\rho(\mathbf{r})$. The variation with respect to $\phi_n^{\sigma*}(\mathbf{r})$ is not equivalent to the variation with respect to the true electronic density. When one kind of $\{\phi_n^\sigma(\mathbf{r})\}$ is chosen, it means that a kind of non-interacting electron is used to describe the real system approximately. This causes two kinds of errors: (i) The calculated E_G and $\rho(\mathbf{r})$ will deviate from the true total energy and electronic density of the real system, respectively. (ii) A single $|\phi_n^\sigma(\mathbf{r})|^2$, and its eigenvalue ϵ_n^σ, will deviate from the probability distribution and energy of a real electron, respectively. The error (ii) can be understood as follows: For a given boundary condition, equation (5) has a unique set of $\{\phi_n^\sigma(\mathbf{r}),\ \epsilon_n^\sigma\}$. If one $\phi_n^\sigma(\mathbf{r})$ is poor for describing a real electron, the kinetic energy of the non-interacting electron represented by the $\phi_n^\sigma(\mathbf{r})$ will be notably different from that of the real electron according to the equation (4). So the eigenstate represented by the $\phi_n^\sigma(\mathbf{r})$ will notably deviate from the state of the real electron.

(IV) Boundary conditions and the symmetry of effective one-electron Hamiltonian. Indicating with $H'_a(\mathbf{r})$ the effective one-electron Hamiltonian containing boundary conditions in equation (5), and with $H_a(\mathbf{r})$ the same but without boundary condition, the symmetries of $H'_a(\mathbf{r})$ and $H_a(\mathbf{r})$ can be either the same or different because there are many physically reasonable boundary conditions. For a crystal, assume that the $H_a(\mathbf{r})$ has the translation symmetry of the crystal. Apply a translation operator to equation (5),

$$\hat{T}_{\mathbf{R}} H'_a(\mathbf{r})\phi^\sigma_n(\mathbf{r}) = \hat{T}_{\mathbf{R}}\epsilon^\sigma_n\phi^\sigma_n(\mathbf{r}). \tag{10}$$

(i) Band structure calculation. Every $\phi^\sigma_n(\mathbf{r})$ is assumed to spread over the whole space and satisfies the periodic boundary condition. So the $H'_a(\mathbf{r})$ and $H_a(\mathbf{r})$ have the same translation symmetry, and equation (10) becomes $H'_a(\mathbf{r})\hat{T}_{\mathbf{R}}\phi^\sigma_n(\mathbf{r}) = \epsilon^\sigma_n\hat{T}_{\mathbf{R}}\phi^\sigma_n(\mathbf{r})$. This means that $\hat{T}_{\mathbf{R}}$ commutes with $H'_a(\mathbf{r})$, and both $\hat{T}_{\mathbf{R}}\phi^\sigma_n(\mathbf{r})$ and $\phi^\sigma_n(\mathbf{r})$ are eigenfunctions having the same eigenvalue ϵ^σ_n. The $\phi^\sigma_n(\mathbf{r})$ can be shown to be Bloch functions, and a single $|\phi^\sigma_n(\mathbf{r})|^2$ and $\rho(\mathbf{r})$ have the same symmetry and distribution region. This is the Bloch theorem. (ii) The SCCE calculation. The $\{\phi^\sigma_n(\mathbf{r})\}$ are assumed to localize in k embedded-cluster regions, and satisfy k special boundary conditions (7) and (8). So the $H'_a(\mathbf{r})$ has no translation symmetry of $H_a(\mathbf{r})$, equation (10) can be written as $[\hat{T}_{\mathbf{R}}H'_a(\mathbf{r})]\hat{T}_{\mathbf{R}}\phi^\sigma_n(\mathbf{r}) = \epsilon^\sigma_n\hat{T}_{\mathbf{R}}\phi^\sigma_n(\mathbf{r})$. Now the $\hat{T}_{\mathbf{R}}H'_a(\mathbf{r})$ and $H'_a(\mathbf{r})$ are effective one-electron Hamiltonians acting on two different embedded-clusters, and $\hat{T}_{\mathbf{R}}\phi^\sigma_n(\mathbf{r})$ and $\phi^\sigma_n(\mathbf{r})$ are eigenfunctions localized in two different embedded-cluster regions but related to the same eigenvalue ϵ^σ_n. The symmetry and distribution region of a single $|\phi^\sigma_n(\mathbf{r})|^2$ are different from that of $\rho(\mathbf{r})$.

(V) It is easy to show that the atomic inner electrons, which are almost absolutely localized (this means the overlaps between the electrons of neighboring atoms are zero), can be well described by $\phi^\sigma_n(\mathbf{r})$, used in free cluster calculation, or in the SCCE calculation. A similar conclusion is valid for band structure calculation [33]. So it is enough to discuss only valence electrons which result in the most important effects on the system properties. In band structure calculations, the trial one-electron wave functions $\phi^\sigma_n(\mathbf{r})$ are spread Bloch functions which are only good for describing real quasi-free valence electrons. While in the SCCE calculations, the localized trial one-electron wave functions are good for describing real localized valence electrons. In this sense, the band structure calculation is the best for the systems containing quasi-free valence electrons; while the SCCE calculation is the best for the systems containing localized valence electrons.

Conclusion: It is the difference of the one-electron wave functions that leads to the different outcomes. For $LaNi_5$, the Ni 3 d and La 5d electrons are well localized, and the valence bands are mainly dominated by the Ni 3d electrons. These localized d electrons can be best described by localized $\phi^\sigma_n(\mathbf{r})$ in the SCCE calculations.

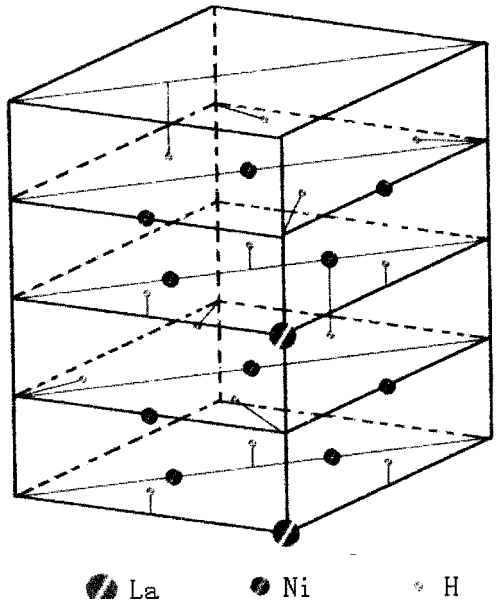

Fig. 3. The embedded-cluster of $(LaNi_5H_7)_2$.

4 Results of $LaNi_5H_7$

The elastic neutron scattering experiments, performed independently by two groups using different samples and different methods [26,27], have reached similar conclusions: the structure of β-$LaNi_5H_7$ can be described by the $P6_3mc$ non-centrosymmetric space group in which the six-fold c axis of the $CaCu_5$ structure has become a 6_3 screw axis because of the ordering of the hydrogen atoms in the planes perpendicular to the c axis. Both results indicate a reduction of symmetry and a doubling of the size of the hexagonal unit cell along the c axis. However, the structural models given by two groups are quite different in detail: (1) Reference [26]. Along the c axis, La and Ni atoms have coordinates of 0, 0.25, 0.5 or 0.75 which mean no displacement, while none of the H atoms have such coordinates. Six from fourteen H atoms have two equal-opportunity positions which are very close. (2) Reference [27]. Along the c axis, Ni atoms have displacements, while the La atoms, and twelve from fourteen H atoms, have coordinates of 0, 0.25, 0.5 or 0.75. All the H atoms have definite positions. We chose the structural model given in reference [26]. The embedded-cluster $(LaNi_5H_7)_2$ is shown in Figure 3. Table 1 gives the fractional coordinates of all 26 atoms in the cluster, where the coordinates of six H atoms (atoms 8, 9, 10, 21, 22, 23) are taken as the averages over the coordinates of two close equal-opportunity positions. We refer the reader to the experimental papers [26,27] for further details concerning the structure.

The cluster $(LaNi_5H_7)_2$ is surrounded by 676 atoms to simulate the β-phase $LaNi_5H_7$. The lattice constants used in our calculation are $a_o = 5.428$ Å and $c_o = 8.627$ Å, which indicate a large lattice expansion compared with $LaNi_5$ ($\Delta a/a_o \approx \Delta c/c_o \approx 8\%$) [27]. The Gaussian bases of Ni and La are the same as that in the $LaNi_5$ cluster. The optimized Gaussian basis set of hydrogen is taken to

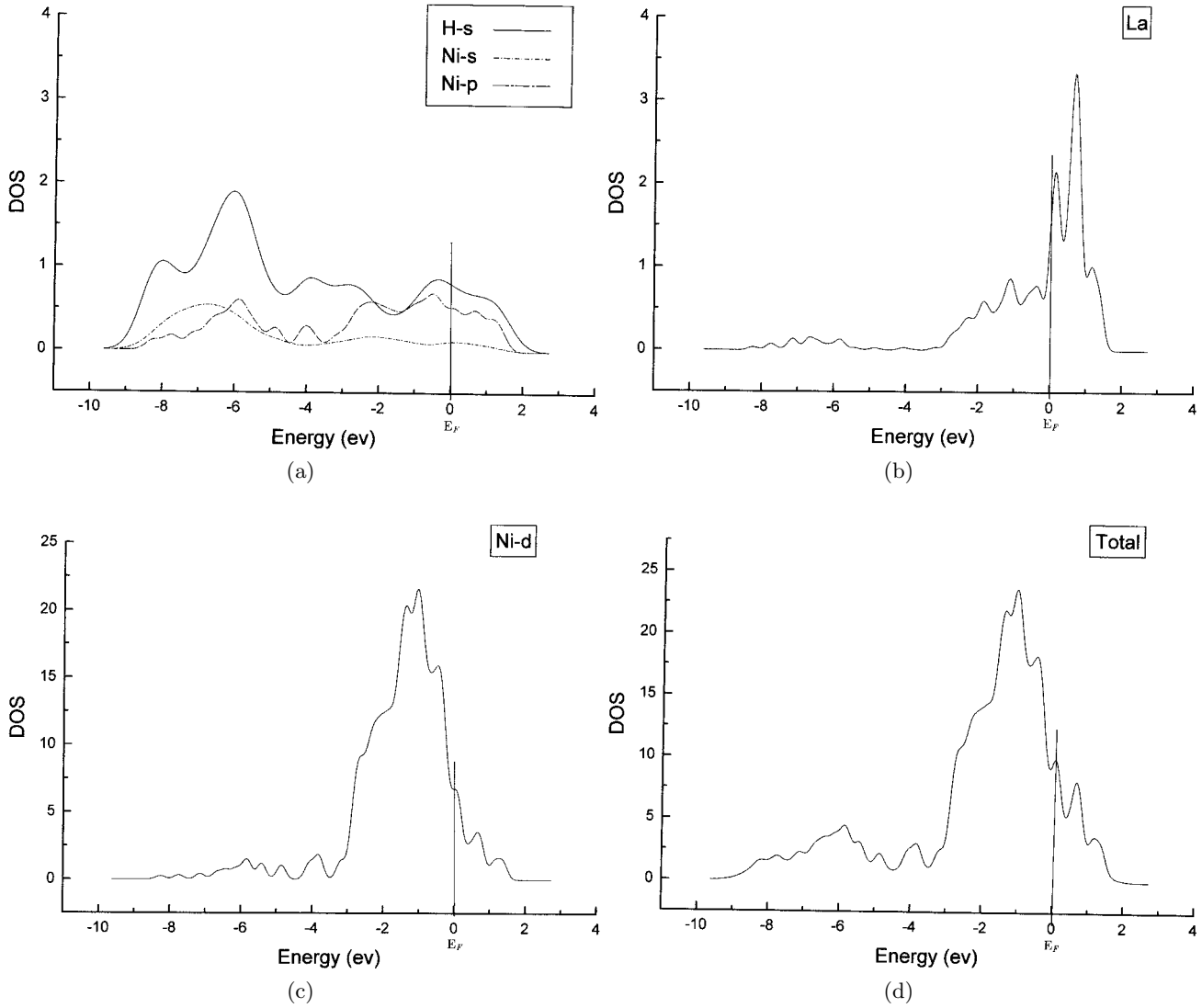

Fig. 4. Density of states of classified spin-up electrons of $LaNi_5H_7$. Units of the DOS are states of per electron-volt per $(LaNi_5H_7)_2$ cell. (a) H-s, Ni-s and Ni-p electrons; (b) La valence electrons; (c) Ni-d electrons; (d) Total spin-up electrons.

be 10s [16]. The total number of Gaussian bases of the embedded-cluster $(LaNi_5H_7)_2$ is 878. There are 2096679 grid points used for the numerical calculation of V_{xc}. After several trial calculations, the optimum values of core radii of surrounding La, Ni and H atoms are: $R_{La} = 1.3499$ a.u., $R_{Ni} = 0.6519$ a.u. and $R_H = 0.5932$ a.u. The total number of cluster-electrons remaining in the core regions of 676 surrounding atoms are 0.0014, which shows that the special boundary condition (7) is well satisfied. Based on the Hellmann-Feynman theory, the total forces acting on each atomic nucleus are calculated. In principle, the total force acting on a nucleus in equilibrium should be zero. In the SCCE calculations, and free-cluster calculations, however, the charge fitting technique is used, which is designed to produce minimum error in electrostatic energy but not charge density [28]. So even for an atom in equilibrium, the calculated total force is not exactly zero but a small value. The last column of Table 1 gives the total forces acting on atomic nuclei (per nuclear charge). They are reasonably small, indicating the atoms are in equilibrium.

There is no spin magnetic moment for the cluster $(LaNi_5H_7)_2$. Figure 4 shows the DOS of spin-up H-s, Ni-s, Ni-p, La ($-s$, $-p$, $-d$), Ni-d and total electrons. The DOS curves of spin down electrons are the same. Each single level has been broadened by a Gaussian function with a FWHM of 1 eV (s electrons), 0.5 eV (p electrons) and 0.3 eV (d electrons), respectively. The contribution of La-s and La-p electrons are negligible. The Fermi level of $LaNi_5H_7$ is $E_F = +0.047$ eV, which falls in a rising portion of the DOS of the lanthanum valence electrons. The total DOS at E_F in the hydride remains large, as observed in $LaNi_5$. The electronic specific-heat coefficient γ is evaluated to be 2.33×10^{-2} J (mole $LaNi_5H_7)^{-1}$ K^{-2}, which is smaller than that of $LaNi_5$. This agrees with the measured

Table 1. Atoms in embedded-cluster $(LaNi_5H_7)_2$.

No.	Atom	Fractional coordinates x (a_o)	y (a_o)	z (c_o)	Total force per nuclear charge (a.u.)
1	La	0	0	0	0.0807
2	Ni	2/3	1/3	0	0.1807
3	Ni	1/3	2/3	0	0.1123
4	Ni	0	1/2	1/4	0.0588
5	Ni	1/2	0	1/4	0.0970
6	Ni	1/2	1/2	1/4	0.0385
7	H	2/3	1/3	0.309	0.0831
8	H	0.147	0.294	0.275	0.0964
9	H	0.706	0.853	0.275	0.0748
10	H	0.147	0.853	0.275	0.0655
11	H	0	1/2	0.060	0.1039
12	H	1/2	0	0.060	0.0843
13	H	1/2	1/2	0.060	0.0267
14	La	0	0	1/2	0.0976
15	Ni	2/3	1/3	1/2	0.0426
16	Ni	1/3	2/3	1/2	0.0672
17	Ni	0	1/2	3/4	0.1114
18	Ni	1/2	0	3/4	0.0770
19	Ni	1/2	1/2	3/4	0.0525
20	H	1/3	2/3	0.809	0.0802
21	H	0.294	0.147	0.775	0.0704
22	H	0.853	0.706	0.775	0.0893
23	H	0.853	0.147	0.775	0.0716
24	H	0	1/2	0.560	0.0775
25	H	1/2	0	0.560	0.0520
26	H	1/2	1/2	0.560	0.0730

value. Ohlendorf and Flotow [23] have observed a small decrease from $\gamma = 4.26 \times 10^{-2}$ J (mole $LaNi_5)^{-1}$ K^{-2} to $\gamma = 4.04 \times 10^{-2}$ J (mole $LaNi_5H_{6.3})^{-1}$ K^{-2}. We observe a small narrowing of the nickel d bands from about 3.0 eV (FWHM) in $LaNi_5$ to about 2.7 eV (FWHM) in $LaNi_5H_7$. This is due in part to the large lattice expansion observed upon hydrogenation and also to the modification of the nickel d bands due to the Ni-H interaction. Our results are in general agreement with the reference [4]. The following characteristics deserve our extra attention.

(A) The major contribution to the valence bands is made by the nickel $3d$ electrons (74.5%) and the hydrogen $1s$ electrons (13.9%). The contribution of lanthanum $5d$ electrons is less than 3.1%. However, the La $5d$ electrons locate mostly near the Fermi level and make a contribution of 14% to the DOS at E_F.

(B) The hydrogen $1s$ electrons are mainly distributed in the energy region of $-2 \sim -8$ eV, where their DOS is comparable to that of nickel valence electrons. The DOS of lanthanum $5d$ electrons, however, is almost zero in this energy region. This indicates that in $LaNi_5H_7$, the hydrogen $1s$ electrons hybridize mainly with nickel valence electrons. In other words, the hydrogen atoms are mainly combined with nickel atoms.

(C) There is a charge transfer from lanthanum to hydrogen: each La atom loses 1.16 electrons, each Ni atom loses 0.05 electrons, and each H atom gets 0.20 electrons. The total number of La electrons in the valence band is 1.83.

(D) If the E_{xc} in equation (1) is considered to be correct, according to Slater and Janak [30–32], the absolute value of an eigenvalue (including the Fermi level) is equal to the amount of energy required to remove an electron from the orbital, with the error being of the second order in the derivative of the total energy. The transition-state method [30–32] will reduce the error to the third order. Our results show that for $LaNi_5H_7$, $E_F = +0.047$ eV, which is unusually high, and is about 5.172 eV higher than that of $LaNi_5$. This means that the $LaNi_5H_7$ is less stabler than $LaNi_5$, perhaps being metastable. The result of transition-state method shows 1.92 eV of ionization potential of the orbital at E_F. Because the surrounding charge density ρ_2 is fixed and the electron rearrangement in embedded-cluster $(LaNi_5H_7)_2$ is limited by ρ_2 in the transition-state method of the SCCE calculation, the ionization potential obtained above is higher than the real value (the limitation of rearrangement raises the energy) [5]. The real ionization potential is estimated to be about 1 eV. This shows that the electron does not easily leave $LaNi_5H_7$. It may be easier for hydrogen atoms to escape.

Because the environmental atoms and the embedded-clusters in two calculations are different, the total energy of the embedded-clusters $LaNi_5$ and $(LaNi_5H_7)_2$ are incomparable. Thus we are unable to explain hydrogenation of $LaNi_5$ by comparing the binding energies. However, compare the results of $LaNi_5$ with that of $LaNi_5H_7$, there are following important characteristics: (i) In both $LaNi_5$ and its hydride $LaNi_5H_7$, the lanthanum 5d electrons are well localized and are located nearby the Fermi level. (ii) $LaNi_5$ has no significant charge transfer from La to Ni, while its hydride $LaNi_5H_7$ has a charge transfer of 1.16 electrons from lanthanum to hydrogen. (iii) In $LaNi_5H_7$, the hydrogen atoms are mainly combined with nickel atoms to form hybridized orbitals in the energy regions lower than that of lanthanum $5d$ electrons. Based on this, we propose the following feature of hydrogenation of $LaNi_5$: It is easy for hydrogens to take off some localized La $5d$ electrons near the Fermi level, and combine with nickel to form hybridized orbitals in lower energy regions. This process is in favor of energy, and forces the lattice expansion until the Fermi level rises to zero. The lanthanum $5d$ electrons act as a catalyst in the hydrogenation of $LaNi_5$. It is interesting to compare this with our previous calculation [8] which reveals that hydrogen can induce vacancy formation in pure Ni metal as suggested by the experiment of Fukai and Okuma [29]. A vacancy can contain six hydrogen atoms which are along the octahedral directions displaced by $a_o/2$ (a_o being the lattice constant of pure Ni) from the vacancy center.

5 Conclusions

Using the self-consistent cluster-embedding method, the electronic structures of $LaNi_5$ and its hydride $LaNi_5H_7$ are obtained by the first principle, all-electron, full-potential calculations. The calculated width of nickel d bands and electronic specific-heat coefficients are in good agreement

with the experimental data. It is found that in both materials, the contribution of La 5*d* electrons to DOS of valence bands are small, but almost all of La 5*d* electrons locate near the Fermi levels. The Fermi level of $LaNi_5H_7$ is close to zero, which is 5.172 eV higher than that of $LaNi_5$. For $LaNi_5$, there is no significant charge transfer from La to Ni. For $LaNi_5H_7$, however, the calculations reveal a charge transfer of 1.16 electrons from La to H. The hydrogens are mainly combined with the Ni in the energy regions far below the Fermi level. From this, an explanation of hydrogenation of $LaNi_5$ is proposed: It is easy for hydrogens to take off some localized La 5*d* electrons near the Fermi level, and combine with Ni to form hybridized orbitals in lower energy regions. This process is in favor of energy, and forces a lattice expansion until the Fermi level rises to zero.

This work was supported by the Foundation of Academy of Engineering and Physics of China under Grant No. 98030910.

References

1. J.H.N. Van Vucht, F.A. Kuijpers, H.C.A.M. Bruning, Philips Res. Rep. **25**, 133 (1970)
2. C.E. Lundin, F.E. Lynch, C.B. Magee, J. Less-Common Met. **56**, 19 (1977)
3. S.K. Malik, F.J. Arlinghaus, W.E. Wallace, Phys. Rev. B **25**, 6488 (1982)
4. M. Gupta, J. Less-Common Met. **130**, 219 (1987)
5. H. Zheng, Phys. Rev. B **48**, 14868 (1993)
6. H. Zheng, Phys. Lett. A **226**, 223 (1997); **231**, 453 (1997)
7. H. Zheng, Physica B **212**, 125 (1995).
8. H. Zheng, B.K. Rao, S.N. Khanna, P. Jena. Phys. Rev. B **55**, 4174 (1997)
9. H. Zheng, Phys. Rev. E **62**, 5500 (2000).
10. P. Hohenberg, W. Kohn, Phys. Rev. **136**, B864 (1964)
11. W. Kohn, L.J. Sham, Phys. Rev. **140**, A1133 (1965)
12. J.H. Wernick, S. Geller, Acta Crystallogr. **12**, 663 (1959)
13. R. Hempelmann *et al.*, J. Less-Common Met. **104**, 1 (1984)
14. J.L. Soubeyroux, A. Percheron-Guegan, J.C. Achard, J. Less-Common Met. **129**, 181 (1987)
15. A.J.H. Wachters, J. Chem. Phys. **52**, 1033 (1970)
16. A.K. Rappe, T.A. Smedley, W.A. Goddard III, J. Phys. Chem. **85**, 2607 (1981)
17. R. Poirier, R. Kari, I.G. Csizmadia, *Handbook of Gaussian Basis Sets* (Elsevier, Amsterdam, 1985)
18. S. Huzinaga, *Gaussian Basis Sets for Molecular Calculations* (Elsevier, Amsterdam, 1984)
19. J.H. Weaver *et al.*, J. Appl. Phys. **51**, 5847 (1980)
20. L. Schlapbach, Solid State Commun. **38**, 117 (1981)
21. S. Nasu *et al.*, J. Phys. Chem. Solids **32**, 2779 (1971).
22. G.J. McCarthy, J.J. Rhyne, H.B. Silber, *The Rare Earths in Modern Science and Technology* (Plenum, New York, 1980), p. 563
23. D. Ohlendorf, H.E. Flotow, J. Chem. Phys. **73**, 2937 (1980)
24. L. Schlapbach, J. Phys. F **10**, 2477 (1980)
25. W.E. Wallace, *Rare Earth Intermetallics* (Academic, New York, 1973), p. 129
26. C. Lartigue *et al.*, J. Less-Common Met. **113**, 127 (1985)
27. P. Thompson *et al.*, J. Phys. F **16**, 675 (1986)
28. H. Sambe, R.H. Felton, J. Chem. Phys. **62**, 1122 (1975)
29. Y. Fukai, N. Okuma, Jpn J. Appl. Phys. **32**, L1256 (1993)
30. J.C. Slater, J.H. Wood, Int. J. Quantum Chem. Suppl. **4**, 3 (1971)
31. J.C. Slater, Adv. Quantum Chem. **6**, 1 (1972)
32. J.F. Janak, Phys. Rev. B **18**, 7165 (1978)
33. T.A. Kaplan, P.N. Argyres, Phys. Rev. B **1**, 2457 (1970)